

Article

Preparation and Emulsifying Properties of Carbon-Based Pickering Emulsifier

Huihui Lv^{1,2}, Zebo Wang¹, Jialong An¹, Zhanfeng Li², Lei Shi³ and Yuanyuan Shan^{1,*}¹ School of Materials Science and Engineering, Taiyuan University of Technology, Taiyuan 030024, China² College of Optoelectronics, Taiyuan University of Technology, Taiyuan 030024, China³ State Key Laboratory of Chemical Resource Engineering, Beijing University of Chemical Technology, Beijing 100029, China

* Correspondence: shanyuanyuan@tyut.edu.cn

Abstract: Water is increasingly being used as a solvent in place of organic solvent in order to meet the demand for green chemical synthesis. Nevertheless, many of the reaction substrates are organic matter, which have low water solubility, resulting in a low reaction interface and limiting the development of organic-water biphasic systems. A surfactant is typically added to the two-phase system to form an emulsion to increase the contact area between the organic phase and the water. Compared to ordinary emulsion stabilized with the surfactant, Pickering emulsion offers better adhesion resistance, biocompatibility, and environmental friendliness. It possesses unrivaled benefits as an emulsifier and catalyst in a two-phase interfacial catalysis system (PIC). In this study, the amine group (NNDB) was employed to alter the surface of graphene oxide (GO). A stable Pickering emulsion was created by adsorbing GO-NNDB on the toluene–water interface. It was determined that the emulsion system had good stability by analyzing digital photographs and microscope images of droplets at various temperatures, and fluorescence microscopy images of emulsion droplets created by both newly added and recovered emulsifiers. This work provided the groundwork for future applications of Pickering emulsion in interfacial catalysis.

Keywords: Pickering emulsion; graphene oxide; interfacial catalysis



Citation: Lv, H.; Wang, Z.; An, J.; Li, Z.; Shi, L.; Shan, Y. Preparation and Emulsifying Properties of Carbon-Based Pickering Emulsifier. *Processes* **2023**, *11*, 1070. <https://doi.org/10.3390/pr11041070>

Academic Editor: Urszula Bazylinska

Received: 12 February 2023

Revised: 12 March 2023

Accepted: 14 March 2023

Published: 2 April 2023



Copyright: © 2023 by the authors. Licensee MDPI, Basel, Switzerland. This article is an open access article distributed under the terms and conditions of the Creative Commons Attribution (CC BY) license (<https://creativecommons.org/licenses/by/4.0/>).

1. Introduction

An emulsion is a system consisting of two insoluble liquids, or when one of the liquids is dispersed in the other. Due to the high surface energy at the interphase interface between two incompatible solutions, the emulsion is thermodynamically unstable. Stable emulsions to facilitate industrial production have been widely studied. Ramsden [1] and Pickering [2] first discovered an emulsion stabilized by solid particles nearly a century ago (Pickering emulsion). The adsorption of the solid particles on the two-phase interface formed a mechanical barrier, and it changed the steric hindrance between the particles and stabilized the Pickering emulsion [3]. Because of the low toxicity, strong interfacial stability, and environmental friendliness of Pickering emulsion, it is widely used in food technology [4,5], wastewater treatment [6], oil recovery [7,8], drug delivery [9], and interfacial catalysis [10].

With the advancement of green chemistry, water from nature has become a popular green solvent to replace organic solvents in reactions [11]. However, because some organic reactants are poorly soluble in water, the contact area between the two phases is minimal, which is detrimental to the reaction [12]. Surfactants are typically required to stabilize the two oil–water phases while creating an emulsion in order to improve the contact area between the two phases [13]. Stabilizing emulsions typically requires a significant quantity of surfactants, which are harmful to both human health and the environment [14]. The use of surfactants will definitely increase the complexity of the reaction system and impair product and emulsifier recovery. Pickering emulsion effectively addresses these issues. In Pickering interfacial catalysis (PIC) systems, Pickering emulsifier

acts as both emulsifier and catalyst at the liquid/liquid interface (L/L). Because of its large reaction interface and unique biphasic environment, the system has irreplaceable advantages in double phase reactions, including (1) excellent solid catalyst recovery performance; (2) large interfacial area to promote reaction kinetics; (3) ability to selectively catalyze different reaction substrates distributed in two immiscible reagents; and (4) spontaneous separation of key products on the basis of a “phase transfer” procedure [15]. In recent years, the PIC system has been widely used in oxidation reactions [16,17], reduction reactions [18], acid-base catalyzed reactions [19], and biocatalytic reactions/enzymatic reactions [20].

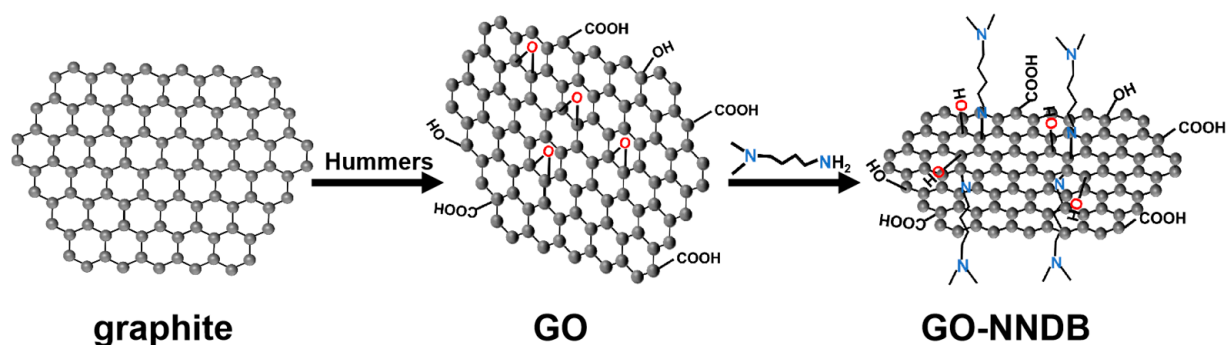
The type and morphology of solid particles can regulate the performance of Pickering emulsions. Specifically, the shape of the particles determines the way they behave at the interface, and this influences their ability to stabilize the emulsion. It is essential to select suitable nano/micro-particles to obtain Pickering emulsions with specific types, characteristics, and applications [21]. Currently, the shapes of solid particles are mainly spherical [22–25], two-dimensional structures [26–29], anisotropic particles [30,31], rod-shaped [32], ellipsoid [33,34], and others.

Graphene oxide (GO) is an ultra-thin flexible sheet of two-dimensional structural material [35] with a high specific surface area. More surfaces can be exposed compared with rigid spherical emulsifiers when adsorbed at the oil/water interface. Moreover, due to GO's high volume/mass ratio, the amount of emulsifier adsorbed on the droplet interface will be reduced significantly. Hence, GO shows unique advantages in emulsion catalysis as a Pickering emulsifier [36].

GO is obtained from the oxidation of graphite powder, which is a derivative of graphene [37]. Due to its unique structure, GO has great potential for the cost-effective large-scale production of graphene-based materials [38,39]. The GO is composed of a two-dimensional lattice with partially broken sp^2 hybridized bonds, with hydroxyl and epoxide groups on the surface and carboxylic acid groups on the edges. This makes GO a certain amphiphilicity (hydrophilic–hydrophobic). The assembly behavior of GO at air–water, liquid–liquid, and liquid–solid interfaces is reported by Kim [40], proving that GO can be used as a colloidal surfactant. Gudarzi and Sharif [41] studied the preparation of polymer/GO microspheres by in-situ polymerization employing GO as a colloidal surfactant. Nanocomposites containing 0.3 wt% graphene showed better thermal stability and stiffness compared with pure resin. Danae [42] utilizes GO of different qualities combined with hexagonal boron nitride nanosheets (h-BNNS). Two different types of emulsion (O/W and W/O) are obtained in the same two-phase system. Their results show a new method for the preparation of graphene/h-BNNS functional materials with novel nanostructures employing a Pickering emulsifier as a soft template. Graphene oxide nanoribbons (GONR) previously obtained by longitudinal cutting of carbon nanotubes (CNTs) were employed as a precursor [43]. A pH-responsive Pickering emulsifier (GONR-IL) was achieved by the amidation of $-NH_2$ in ionic liquid (IL) with $-COOH$ on the GONR surface. Compared with GO-IL emulsifier obtained by a combination of GO and IL, higher stability and smaller emulsion drop size can be obtained by Pickering emulsion stabilized by GONR-IL at the toluene–water phase interface. Moreover, Pd/GONR-IL prepared by GONR-IL as an emulsion catalyst for benzyl alcohol oxidation indicates excellent catalytic activity (the conversion rate can reach 92% in 3 h of reaction). The emulsion catalyst following the reaction can be demulsified and recovered by adjusting the pH. Due to these properties, the emulsion catalyst has broad application prospects in the field of biphasic catalysis. In spite of previous studies on the preparation of GO emulsifiers, the emulsifying ability of emulsifiers and the interface area of emulsions need to be further enhanced.

In this paper, a Pickering emulsifier (GO-NNDB) with excellent wettability is obtained by a ring-opening reaction between the amine group (*N,N*-dimethyl-1,4-butanediamine, NNDB) and the epoxy group on the GO surface. The synthetic route of GO-NNDB is shown in Scheme 1. This Pickering emulsifier leads to the stabilization of the toluene–water biphasic interface over a wide range of ratios. The emulsion system has good stability, and the optimum emulsifying conditions are achieved by adjusting the volume ratio of toluene

to water as well as the concentration of the emulsifier. The mechanism of emulsion stability was examined by contact angle characterization of GO and GO-NNDB. The emulsion created under ideal emulsification conditions can be stable at ambient temperature for two months and can be heated at 85 °C for five hours while staying stable. The successful development of GO-NNDB set the groundwork for its subsequent use in PIC systems.



Scheme 1. Preparation of GO-NNDB.

2. Materials and Methods

2.1. Material and Reagent

Graphite (<20 μm , >99.5%), potassium permanganate (>99.0%), concentrated sulfuric acid (>95.0%), hydrochloric acid (36–38%), and toluene ($\geq 99.5\%$) were purchased from Sinopsin Chemical Reagent Co., Ltd. (Shanghai, China); sodium hydroxide (>96.0%), sodium nitrate (98%), and *N,N*-dimethyl 1,4-butylenediamine ($\geq 95\%$) from Aladdin Biotechnology (Shanghai, China); Hydrogen peroxide (30%) was purchased from Albokai Chemical Co., Ltd. (Tianjin, China). In this study, all reagents used were of analytical grade.

2.2. Preparation of Materials and Emulsions

2.2.1. Preparation of GO

GO was prepared by an improved Hummers method. At first, 5 g of graphite and 2.5 g of NaNO_3 were added into 130 mL of concentrated sulfuric acid, stirred in an ice bath for 2 h, and then 15 g of KMnO_4 was added slowly into the reaction system. Then, the above suspension was transferred to a 35 °C water bath. Further, 230 mL of deionized water was added slowly and stirred continuously for 1 h. The temperature of the water bath was set at 98 °C. It was stirred for 30 min before turning off the heat. The unreacted potassium permanganate was removed by adding 400 mL of deionized water and 10 mL of hydrogen peroxide to the system. After standing, the product was centrifuged to neutral with deionized water to remove the remaining water-soluble ions in the GO stock solution. We stored the product in a silk bottle for later use.

2.2.2. Preparation of GO-NNDB

In total, 160 mg of NaOH was added after dispersing 5 mL of GO in 40 mL of deionized water. The mixture was stirred for 10 min, and then ultrasonically dispersed for 30 min, followed by A reaction at 70 °C for 3 h after adding 515 μL NNDB. After the reaction, the mixture was cooled to room temperature, centrifuged, and washed until neutral. The final product (GO-NNDB) was then cold-dried for use.

2.2.3. Preparation of Pickering Emulsion

Place a certain amount of dried GO-NNDB in a 15 mL glass bottle. Add deionized water and ultrasonic for 30 min to make GO-NNDB evenly dispersed in water. Toluene was added to the above dispersing solution and emulsified for 2 min (10,000 r) with a high-speed shear machine. After standing for 5 min, it was observed under a microscope and pictures were taken.

2.3. Emulsion Stability Test

2.3.1. Thermal Stability Test

Place 5 portions of 12 mg dried GO-NNDB in 15 mL glass bottles with 4 mL deionized water. After each 30 min ultrasound, 8 mL toluene was added to each glass bottle and emulsified for 2 min (10,000 r) with a high-speed shear. After standing for 5 min, the 5 glass bottles were placed in a constant temperature water bath at 25 °C, 45 °C, 65 °C, 85 °C, and 100 °C, and removed after 5 h. After standing for 5 min, the glass bottles were observed under a microscope and pictures were taken.

2.3.2. Stability Test

Place 12 mg of dried GO-NNDB in a 15 mL glass bottle with 4 mL of deionized water. Then, 30 min after ultrasound, 8 mL toluene was added into glass bottles and emulsified for 2 min (10,000 r) with a high-speed shear. At 1, 2, 4, 8, and 60 days, the emulsion was observed by optical microscope and photographed. Random statistics of 100 droplet diameters under different standing time can obtain the image of the change of the average droplet diameter with time.

2.4. Determination of Emulsion Type

Place 12 mg of dried GO-NNDB in a 15 mL glass bottle with 4 mL of deionized water. Then, 30 min after ultrasound, 8 mL toluene dissolved with Nile red stain, which was added to the glass bottle and emulsified for 2 min (10,000 r) with a high-speed shear. After standing for 5 min, they were observed by fluorescence microscope and pictures were taken.

2.5. Materials Characterization

We examined the morphology of the materials by using field emission scanning electron microscopy (Bruker QUANTAX) with an accelerating voltage of 10 kV at the same magnification. The FT-IR spectra of the materials were recorded by employing JASCO FT/IR-430 spectrometer with a resolution of 2 cm^{-1} (KBr pellet, carbon loading of $\approx 0.5\text{ wt}\%$). The chemical composition was determined by XPS with Al $K\alpha$ radiation (AXIS SUPRA). The C 1s peak at 284.8 eV was taken as a calibration peak. The pass energy values of 160 and 20 eV were set, respectively, for the survey spectra and the single-element spectra. The water contact angles of the materials were measured on a contact angle measuring instrument (SINDIN CSCDIC-100). The quantitative sample is pressed into as thin slices as possible (about 40 Mpa, thickness about 1 mm) on a tablet press before measurement. The morphology of the water drop after contact with the sample was quickly photographed and recorded. The morphology of emulsion was observed by optical microscope (OLYMPUS-CX33). After the emulsion stood for 5 min, a drop of emulsion was put on the slide, wiped clean in advance, and then observed and photographed. The emulsion was dripped onto a pre-placed slide and then diluted with methyl orange water solution. The type of emulsion was observed with a fluorescence microscope (OLYMPUS SB-X53).

3. Results and Discussion

3.1. Characterization of Emulsifiers

3.1.1. SEM/EDS

From the SEM image of GO in Figure 1, we observe that GO prepared by us is a kind of flexible sheet material. It is shown from EDS images that elements C and O are evenly distributed on the GO surface. Figure 2 reveals that the GO-NNDB obtained after the reaction can still maintain the sheet structure of GO, which indicates that GO has good stability in the modification process. It is shown by the EDS analysis of GO-NNDB that C, O, and N elements were uniformly distributed on the GO surface. This means that NNDB successfully modified the GO surface.

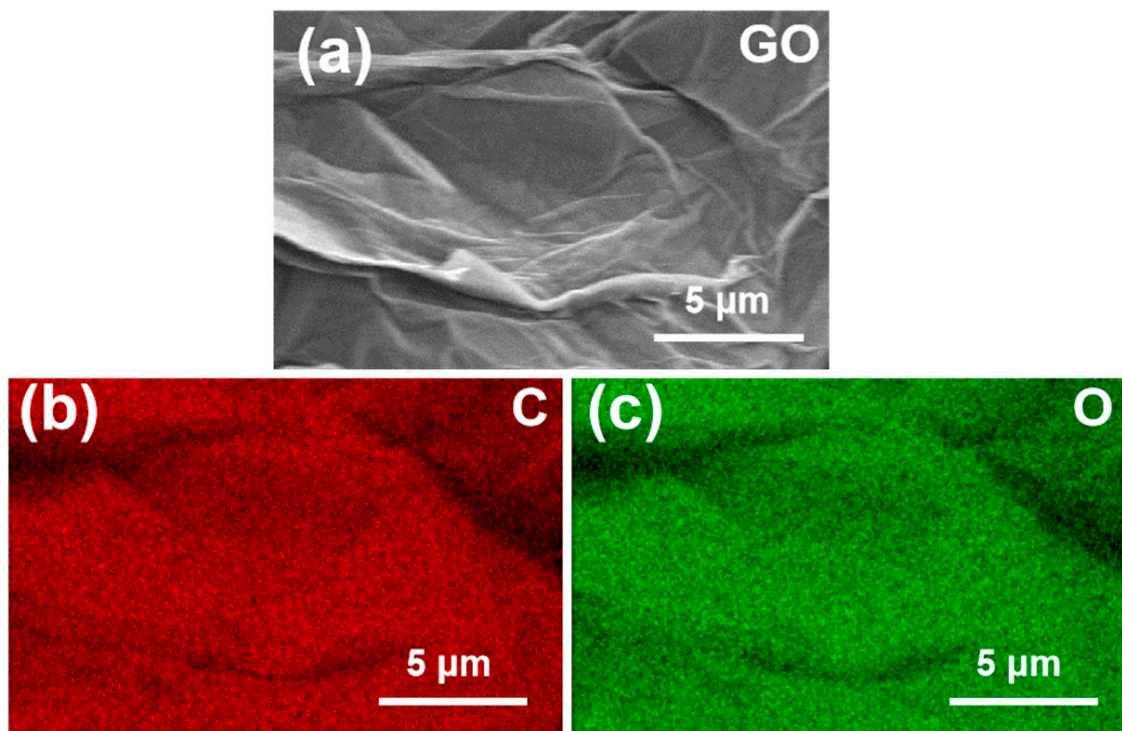


Figure 1. (a) SEM image of GO; EDS characterization of element (b) C, and (c) O.

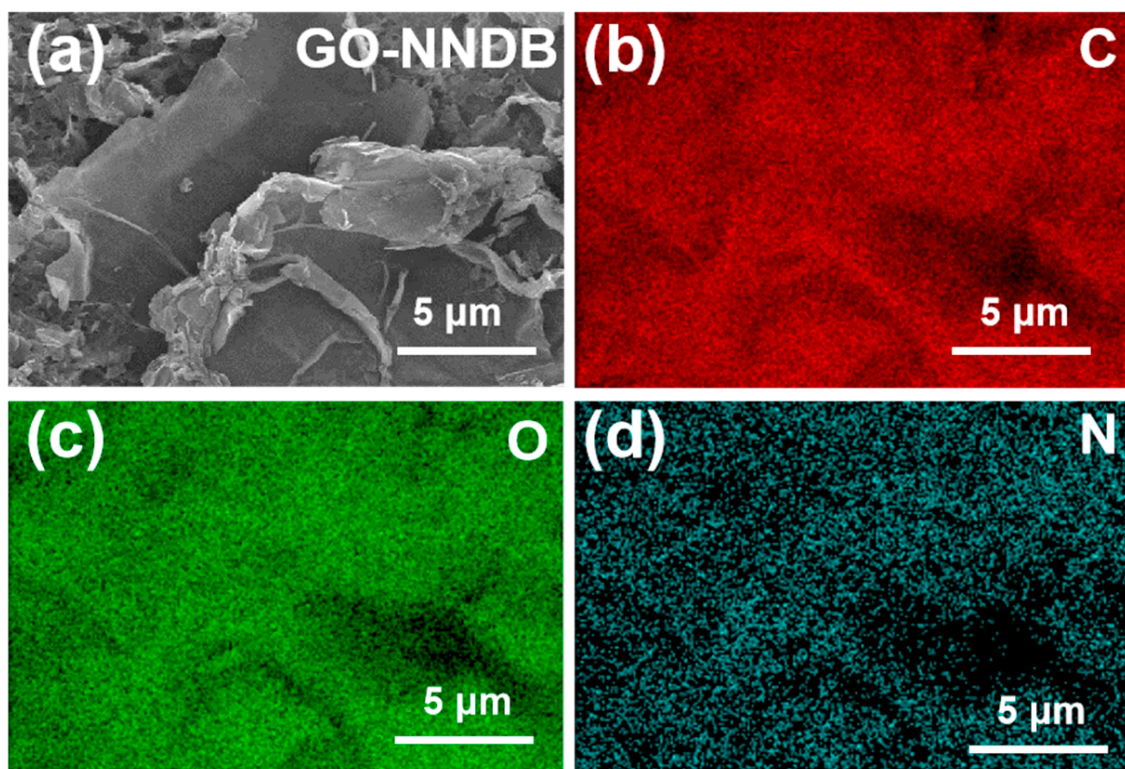


Figure 2. (a) SEM image of GO-NNDB; EDS characterization of element (b) C, (c) O, and (d) N.

3.1.2. FT-IR

To verify that the action mode of NNDB and GO is chemical bonding rather than simple physical adsorption, we employed FT-IR spectroscopy to characterize the surface properties of the materials. Figure 3 shows that the surface of GO prepared by the Hummer

method contains oxygen-containing functional groups, including -OH (3410 cm^{-1}), C=O (1730 cm^{-1}), and C=C (1625 cm^{-1}). It is consistent with what was reported in the previous article [44], which makes surface functionalization modification possible. The NNDB showed characteristic double peaks of symmetric and asymmetric N-H stretching vibrations typical of primary amines at 3296 cm^{-1} and 3373 cm^{-1} (Figure 3a). The double-peaks stretching vibration disappeared during modification, and the stretching vibration peak of C-N appears at 1263 cm^{-1} of GO-NNDB (Figure 3b) during modification. This reveals that NNDB exists on the GO surface [45]. Clearly, the interaction mode of NNDB and GO tends to be the chemical reaction between NNDB and the epoxy group on the GO surface instead of the simple physical adsorption [46,47].

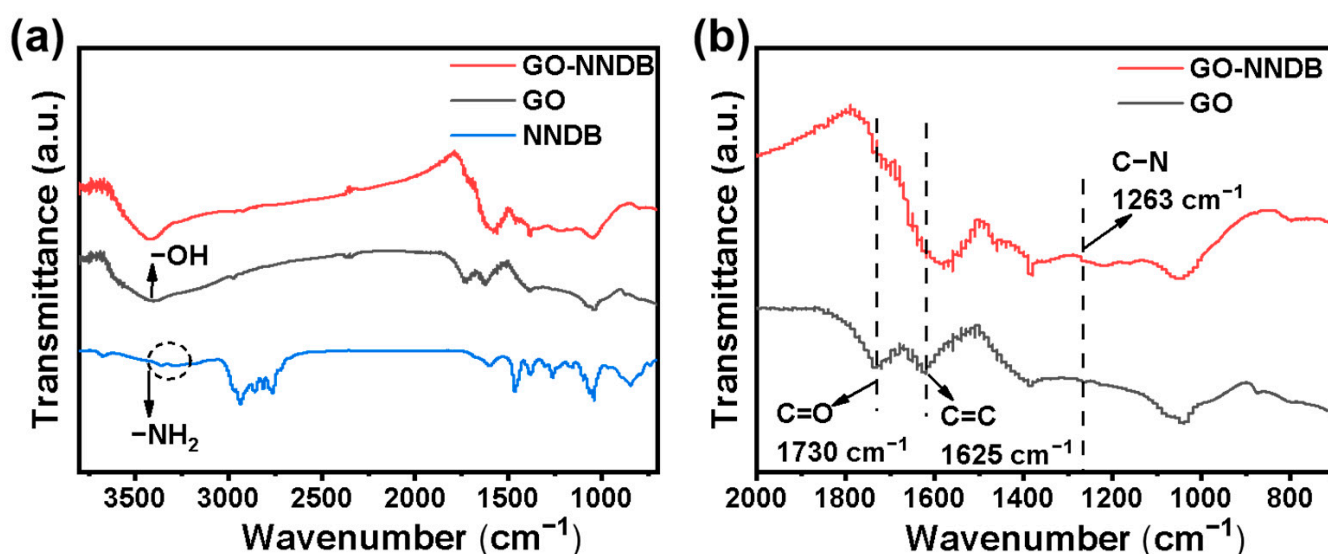


Figure 3. (a) Infrared spectra of GO, GO-NNDB, and NNDB; (b) 700–2000 cm^{-1} infrared magnification image of GO and GO-NNDB.

3.1.3. XPS

To further investigate the surface properties of the materials and the bonding mode, the element types and bonding modes on GO and GO-NNDB surfaces were analyzed by XPS. The XPS spectral comparison of GO and GO-NNDB is shown in Figure 4a. The original GO only revealed typical characteristic peaks of C 1s and O 1s , and the intensity of the O 1s peak was close to that of the C 1s peak. This was caused by the abundant oxygen-containing functional groups on the surface of GO. We note that a new N 1s characteristic peak appeared in the GO-NNDB obtained after NNDB grafting. This means that the grafting process successfully introduced NNDB to the GO surface. For its further peaks shown in Figure 4b, we noted that the binding energy of 399.8 eV and 401.8 eV correspond to the characteristic peaks of secondary and tertiary amine N. Combined with the FT-IR images of NNDB, GO, and GO-NNDB (Figure 3a), the double-peaks of -NH_2 (3296 cm^{-1} , 3373 cm^{-1}) stretching vibration in NNDB disappear during modification, indicating that NNDB has an open-loop reaction through -NH_2 and the C-O-C bond on the GO surface. We observe that a new characteristic peak of the C-N bond appears at 285.5 eV for GO-NNDB by comparing the characteristic peaks of GO and C 1s (Figure 4c,d). This is accompanied by a significant reduction in the content of the C-O bond, which also shows that GO-NNDB is obtained by a ring-opening reaction with the epoxy group on the surface of GO. The above results verified our GO-NNDB preparation scheme.

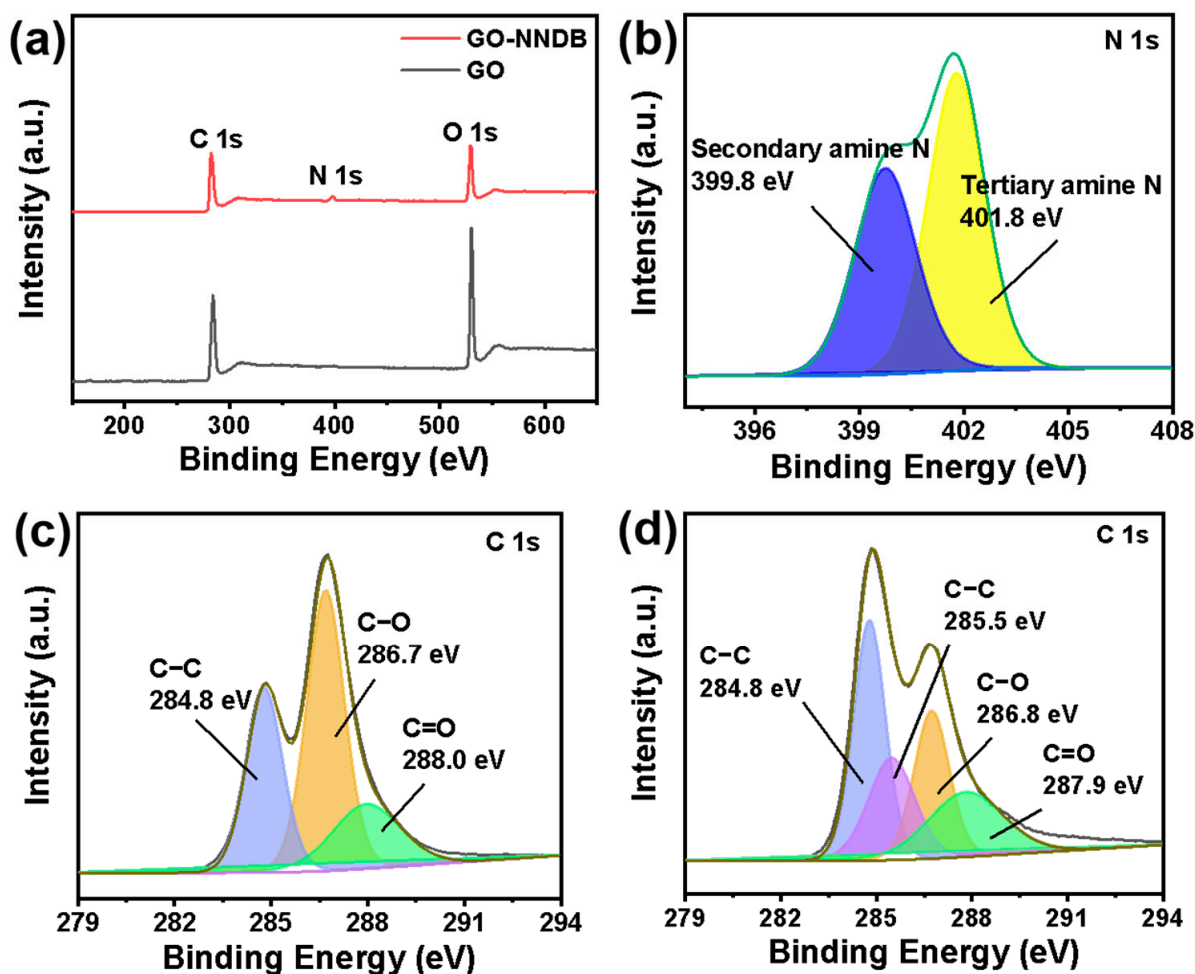


Figure 4. (a) XPS spectra of GO-NNDB and GO; (b) N 1s energy spectrum of GO-NNDB; high resolution C 1s spectra of (c) GO and (d) GO-NNDB.

3.2. Emulsion Effect Optimization

The ratio of toluene to water volume and the concentration of emulsifier are closely related to the stability of the emulsion. To obtain the most suitable toluene–water volume ratio of GO-NNDB as an emulsifier, we investigated the emulsion formed by employing a series of emulsifier concentrations at different toluene–water volume ratios. Figure 5 shows that the emulsion cannot be fully emulsified when the volume ratio of toluene to water is 1:1 and the emulsifier concentration is 0.25–1.5 mg mL^{−1}. When the ratio of toluene to water volume increases to 2:1 and 3:1, and the concentration of emulsifier reaches 0.5 mg mL^{−1}, the emulsion can be fully emulsified. In light of the impact of toluene on the environment, we selected the toluene phase volume as small as possible in this study, so the optimal toluene–water volume ratio was 2:1.

To determine the optimal emulsifier concentration, an optical microscope was used to observe the emulsion formed by different emulsifier concentrations. In Figure 6, we show that a stable emulsion can be formed with an emulsifier concentration of 0.25–1.5 mg mL^{−1}. Another important factor affecting the stability of the emulsion is the size distribution of the emulsion droplets. We carried out the size distribution statistics of emulsion droplets formed by different emulsifiers. The results are shown in Figure 7. Droplet size distribution as a whole becomes more uniform with the increase of emulsifier concentration. Furthermore, the unit mass interface area and the total interface area of the emulsion greatly influence the overall stability of the emulsion and the application of the emulsion in subsequent industrial production. Generally, the smaller the interface area per unit mass, the more microreactors can be provided for interfacial catalytic reactions. The larger the

total interfacial area, the smaller the mass transfer resistance of the two phases, and the more favorable it is to the two phases. We calculated the emulsion interface area per unit mass and total emulsion interface area formed by different emulsifier concentrations. The formulas for calculating the emulsion interface area S and the emulsifying interface area S_m (interface area per unit mass) formed by emulsifier are shown in Equations (1) and (2).

$$S = \frac{6a \cdot V_e}{D} \quad (1)$$

$$S_m = \frac{6a \cdot V_e}{D \cdot m} \quad (2)$$

where a is the utilization rate of milk droplet accumulation space (74%, which is considered as hexagonal dense accumulation), V_e is the volume of emulsion formed, D is the average diameter of droplets, and m is the mass of the emulsifier. The result is shown in Figure 8. We observed that the interface area of the emulsion gradually increases with the increase of emulsifier concentration. Moreover, the interface area per unit mass increases first and then decreases. A total of 1 mg mL^{-1} was determined as the best emulsifier concentration in light of the influence of the emulsion interface area and unit mass interface area.

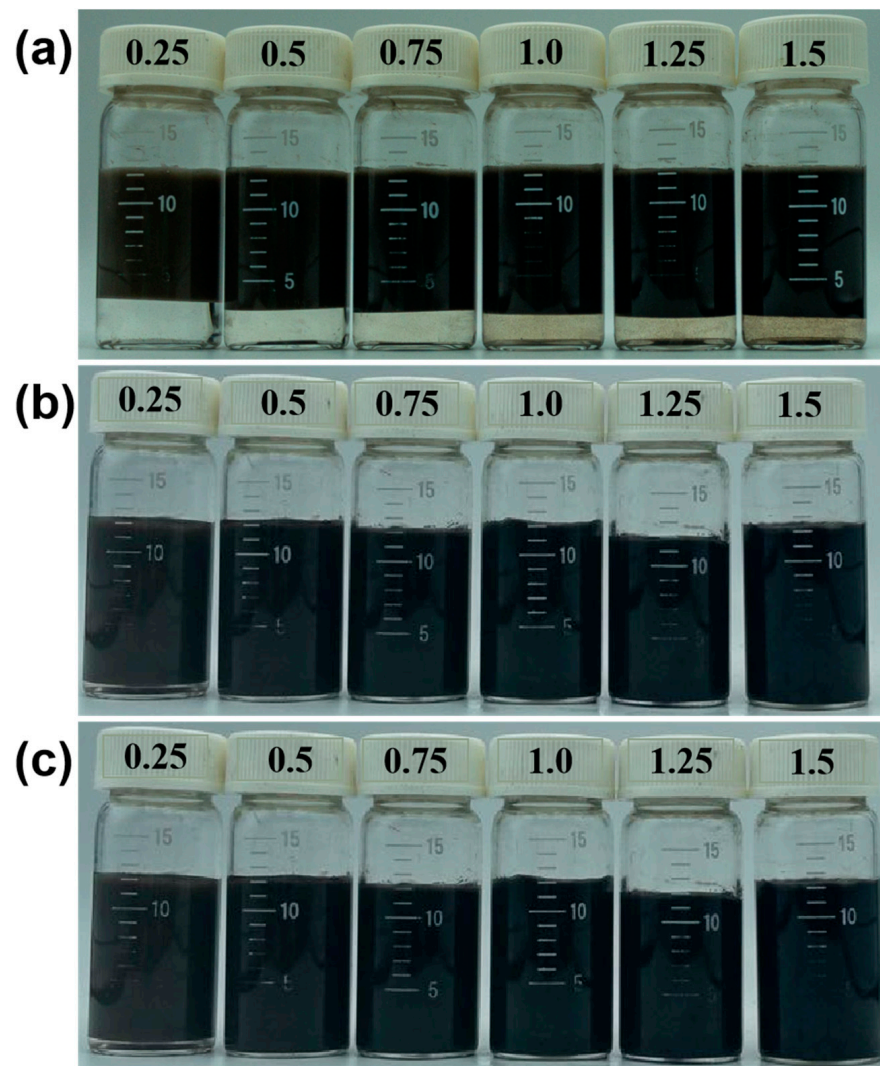


Figure 5. Digital photos of emulsion concentrations (ratio of dry GO-NNDB to total volume of toluene and water) at different toluene–water volume ratios; (a) 1:1; (b) 2:1; (c) 3:1.

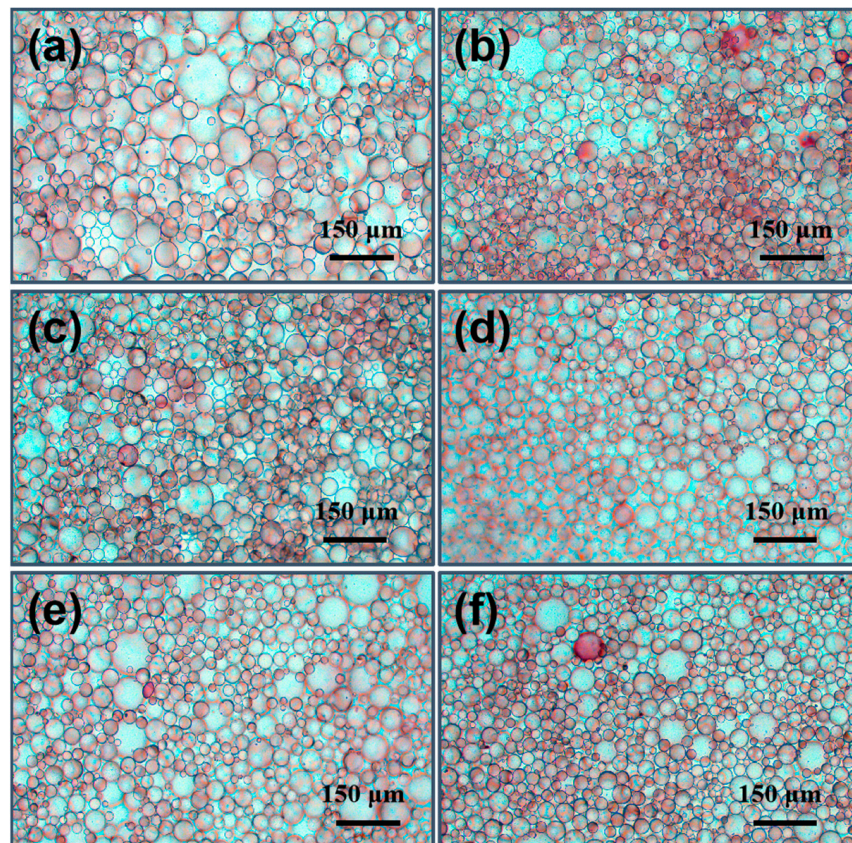


Figure 6. Emulsion microscope images at different concentrations (a–f: 0.25, 0.50, 0.75, 1.00, 1.25, 1.50 mg mL^{-1} , respectively) when the toluene–water volume ratio was 2:1.

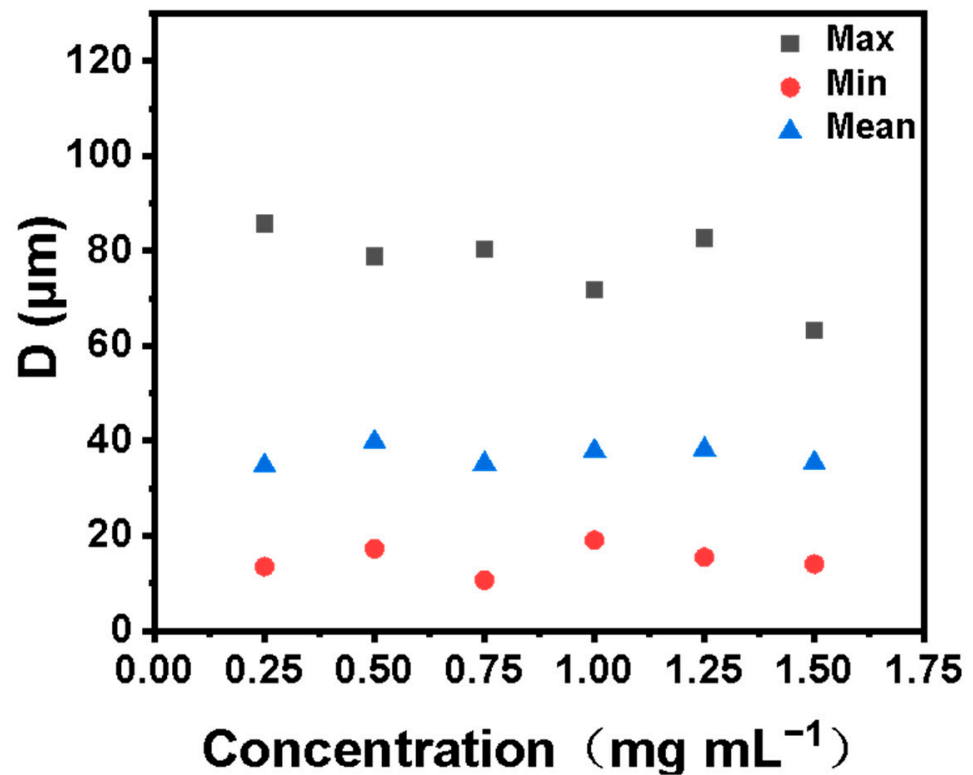


Figure 7. Comparison of emulsion droplet sizes formed by different emulsifier concentrations.

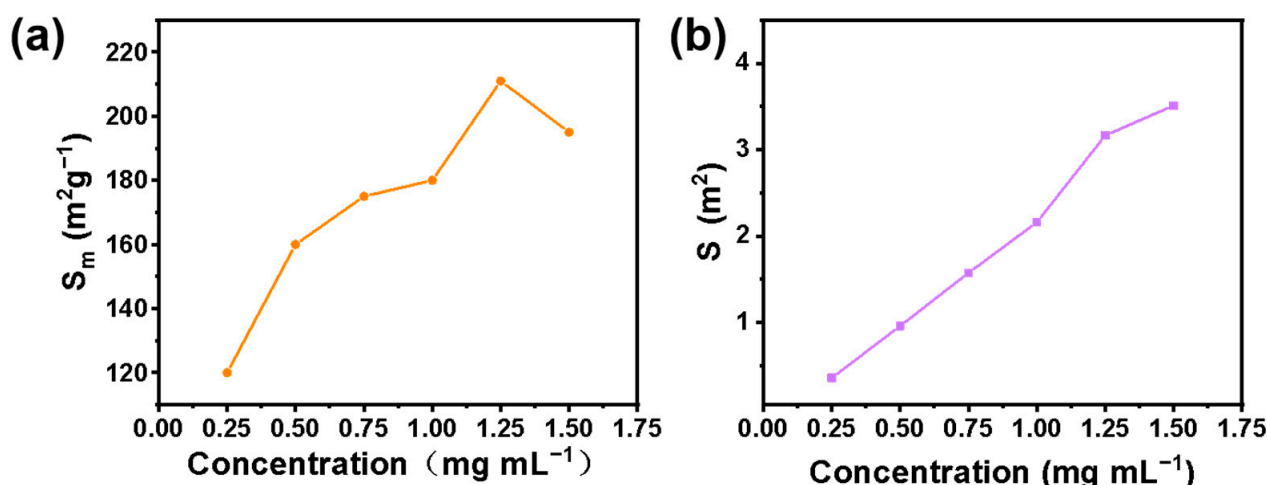


Figure 8. Interface area per unit mass (a) and total interface area (b) of emulsion formed by different emulsifier concentrations.

3.3. Emulsion Stability

It is known that Pickering emulsion with good thermal stability can be better used in a variety of double-phase reactions. In order to investigate the stability of the Pickering emulsion formed by GO-NNDB, the emulsions were first heated at different temperatures (25–100 °C) for 5 h and photos were taken to record the emulsion status. The average size of liquid droplets under the optical microscope was statistically analyzed, and the results are shown in Figure 9a. The average size of the emulsion drops increases gradually, but no obvious demulsification occurs below 85 °C. However, partial demulsification occurs when the temperature is 100 °C, indicating that the emulsion can remain stable at 85 °C for 5 h. Secondly, we recorded the emulsion state and the average size of liquid droplets at different standing times at room temperature (Figure 9b). With the extension of time, the emulsion state did not change significantly, and the average size of the liquid droplets increased only slightly. The results showed that the emulsion could be stable at room temperature for 60 days. Finally, after recovering the emulsifier (GO-NNDB) from the emulsion, GO-NNDB was re-used to stabilize the emulsion (consistent with the method used for the first emulsion preparation). The fluorescence microscope images of the emulsion after five repeated operations and the emulsion formed for the first time are shown in Figure 9c,e (the toluene phase was dyed with Nile red in advance). It was observed that the emulsion type was toluene-in-water, and there was no change after five cycles. As shown in Figure 9d,f, the histogram of emulsion size distribution obtained by statistical analysis of the particle size of liquid droplets shows that the average emulsion size increases only by 0.87 μm. The above results prove that GO-NNDB-stabilized Pickering emulsion has excellent stability.

Binks [48] proposed the desorption energy theory to explain the influence of the surface wettability of solid particles on emulsion stability. The stability of solid particles on the emulsion surface depends on the energy required to transfer from the oil–water interface to the continuous phase. Without considering the interaction force between particles, the formula for calculating desorption energy ΔE in the Pickering emulsion system is shown in Equation (3):

$$\Delta E = \pi R^2 \sigma (1 - |\cos \theta|)^2 \quad (3)$$

In the formula, θ represents three-phase contact antennae; R is particle radius; and σ is interfacial tension.

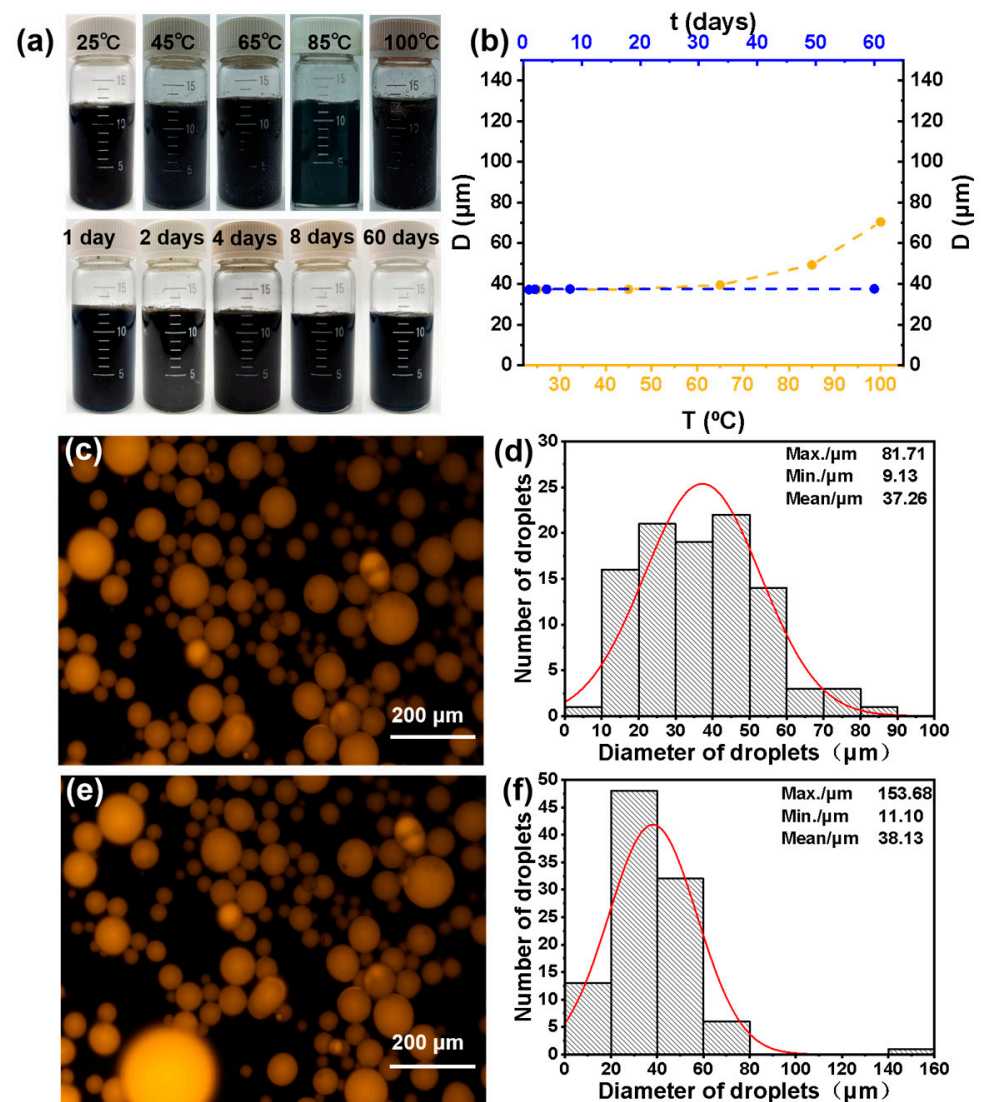


Figure 9. (a) Digital photograph of emulsions at different temperatures and room temperature for different standing times; (b) image of emulsion average droplet size variation with standing time and heating temperature at room temperature; (c) fluorescence microscope images of original emulsion and (d) the corresponding size distribution histogram; (e) fluorescence microscope images, and (f) size distribution histogram after 5 re-emulsification cycles.

According to the formula, when the particles tend to be completely hydrophilic ($\theta = 0^{\circ}$) or completely hydrophobic ($\theta = 180^{\circ}$), the desorption energy is minimum and the emulsion cannot be formed. The closer the θ is to 90° , the better wettability of the particles, the greater the desorption energy, and the more stable the Pickering emulsion obtained.

In order to study the reason why the emulsion formed by GO-NNDB has good stability, we tested the contact angle of GO and GO-NNDB. As shown in Figure 10, the water contact angle of GO is 34° and it has good hydrophilicity. Because there are many oxygen-containing functional groups on the surface of GO, the contact angle of GO-NNDB increases to 88° , which is caused by the modification of the GO surface by NNDB as a hydrophobic molecule. Combined with the desorption energy theory, it can be known that GO-NNDB with a contact angle of 88° has good wettability, thus forming a stable Pickering emulsion.

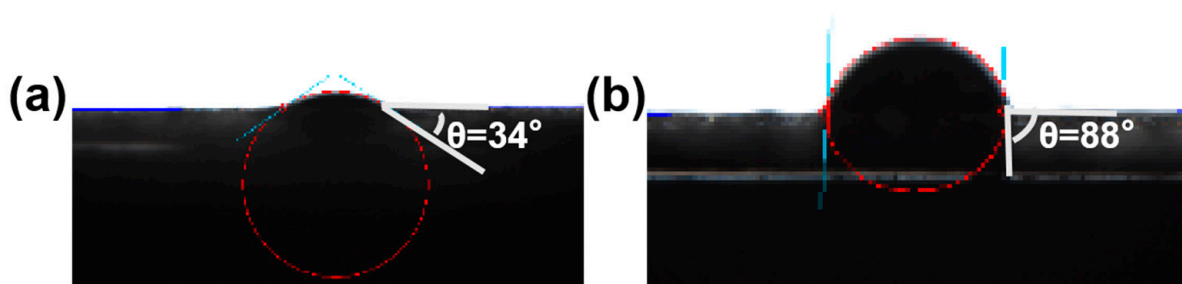


Figure 10. Water contact Angle of GO (a) and GO-NNDB (b).

4. Conclusions

In this paper, we designed and prepared a new type of carbon-based emulsifier by modifying the surface of graphene oxide. Various characterizations indicated that the amino group was successfully grafted onto GO. The amino group is bound to GO by forming a new C–N bond instead of simple physical adsorption. The prepared emulsifier reveals good emulsifying performance. We observe that the emulsion has the best stability when the toluene–water volume ratio is 2:1. It is shown that the optimal emulsifier concentration tends to be 1 mg mL^{-1} based on calculating the interface area per unit mass and the total interface area of the emulsion. Moreover, the emulsion prepared in this work can maintain good dispersion and droplet size under $85 \text{ }^\circ\text{C}$ as well as long-time storage. Fluorescence microscopy showed that GO-NNDB could still be emulsified five times after recovery, and the emulsion type did not change. Studies show that the good stability of the emulsion is attributable to the good wettability of GO-NNDB. However, Pickering emulsion stabilized by GO-NNDB at the toluene–water two-phase interface is only suitable for double phase reactions below $85 \text{ }^\circ\text{C}$, and its application to emulsifiers at higher temperatures needs further study. More importantly, graphite material also has certain toxicity [49]. Although GO-NNDB can be separated from the Pickering emulsion by centrifuge, there will still be some losses in the recovery process. Therefore, it is necessary to further modify GO-NNDB to obtain a Pickering emulsifier that can be efficiently recovered with simple stimulation. In summary, we designed and prepared a recyclable carbon-based Pickering emulsifier that has good stability and can be reused repeatedly. It lays a foundation for the subsequent application of this emulsifier in double phase reactions. It is hoped that the emulsion prepared here can be widely used in the field of green chemistry.

Author Contributions: Conceptualization, H.L. and Y.S.; methodology, Z.W.; validation, Y.S.; formal analysis, H.L.; investigation, Z.W.; data curation, H.L. and J.A.; writing—original draft preparation, H.L. and Z.W.; writing—review and editing, Y.S. and L.S.; supervision, Y.S. and Z.L.; project administration, Y.S.; funding acquisition, Y.S. All authors have read and agreed to the published version of the manuscript.

Funding: This research was funded by Applied Basic Research Programs of Shanxi, grant number 201901D1211098, Funder: Science and Technology Department of Shanxi Province.

Data Availability Statement: Not applicable.

Conflicts of Interest: The authors declare no conflict of interest.

References

1. Ramsden, W. Separation of Solids in the Surface-Layers of Solutions and ‘Suspensions’ (Observations on Surface-Membranes, Bubbles, Emulsions, and Mechanical Coagulation)—Preliminary Account. *Proc. R. Soc. London* **1903**, *72*, 156–164.
2. Pickering, S.U. Cxcvi. *J. Chem. Soc. Trans.* **1907**, *91*, 2001–2021. [[CrossRef](#)]
3. Bizmark, N.; Ioannidis, M.A. Ethyl cellulose nanoparticles at the alkane–water interface and the making of Pickering emulsions. *Langmuir*. **2017**, *33*, 10568–10576. [[CrossRef](#)] [[PubMed](#)]
4. Zhang, X.; Wang, D.; Liu, S.; Tang, J. Bacterial Cellulose Nanofibril-Based Pickering Emulsions: Recent Trends and Applications in the Food Industry. *Foods* **2022**, *11*, 4064. [[CrossRef](#)]

5. Klojdrová, I.; Stathopoulos, C. The potential application of Pickering multiple emulsions in food. *Foods* **2022**, *11*, 1558. [[CrossRef](#)] [[PubMed](#)]
6. Gricius, Z.; Øye, G. Recent advances in the design and use of Pickering emulsions for wastewater treatment applications. *Soft Matter* **2023**, *19*, 818–840. [[CrossRef](#)]
7. Fu, L.P.; Ma, Q.L.; Liao, K.L.; Bai, J.M. Application of Pickering emulsion in oil drilling and production. *Nanotechnol. Rev.* **2022**, *11*, 26–39. [[CrossRef](#)]
8. Tian, Y.; Zhou, J.J.; He, C.Q.; He, L.; Liu, X.G.; Sui, H. The Formation, Stabilization and Separation of Oil–Water Emulsions: A Review. *Processes* **2022**, *10*, 738. [[CrossRef](#)]
9. Peito, S.; Peixoto, D.; Ferreira-Faria, I.; Margarida, M.A.; Margarida, R.H.; Francisco, V.; Marto, J. Nano-and microparticle-stabilized Pickering emulsions designed for topical therapeutics and cosmetic applications. *Int. J. Pharmaceut.* **2022**, *615*, 121455. [[CrossRef](#)]
10. Lv, G.J.; Wang, F.M.; Zhang, X.B.; Binks, B.P. Surface-active hollow titanosilicate particles as a Pickering interfacial catalyst for liquid-phase alkene epoxidation reactions. *Langmuir* **2018**, *34*, 302–310. [[CrossRef](#)]
11. Clarke, C.J.; Tu, W.C.; Levers, O.; Hallett, J.P.; Brohl, A. Green and sustainable solvents in chemical processes. *Chem Rev.* **2018**, *118*, 747–800. [[CrossRef](#)] [[PubMed](#)]
12. Chen, S.; Yan, S.; Zou, H.B.; Xue, N.; Yang, H.Q. Janus mesoporous silica nanosheets with perpendicular mesochannels: Affording highly accessible reaction interfaces for enhanced biphasic catalysis. *Chem. Commun.* **2018**, *54*, 10455–10458.
13. Leclercq, L.; Nardello-Rataj, V. Pickering emulsions based on cyclodextrins: A smart solution for antifungal azole derivatives topical delivery. *Eur. J. Pharm. Sci.* **2016**, *82*, 126–137. [[CrossRef](#)]
14. Ni, L.; Yu, C.; Wei, Q.B.; Qiu, J.S.; Liu, D.M. Pickering emulsion catalysis: Interfacial chemistry, catalyst design, challenges, and perspectives. *Angew. Chem. Int. Edit.* **2022**, *61*, e202115885. [[CrossRef](#)]
15. Wei, Q.B.; Yu, C.; Song, X.D.; Zhong, Y.P.; Ni, L.; Ren, Y.W.; Guo, W.; Yu, J.H.; Qiu, J.S. Recognition of water-induced effects toward enhanced interaction between catalyst and reactant in alcohol oxidation. *J. Am. Chem. Soc.* **2021**, *143*, 6071–6078. [[CrossRef](#)] [[PubMed](#)]
16. Ding, Y.; Xu, H.; Wu, H.H.; Wu, P.; He, M.Y. An amphiphilic composite material of titanosilicate@ mesosilica/carbon as a Pickering catalyst. *Chem. Commun.* **2018**, *54*, 7932–7935. [[CrossRef](#)] [[PubMed](#)]
17. Zhang, Y.B.; Ettelaie, R.; Binks, B.P.; Yang, H.Q. Highly selective catalysis at the liquid–liquid interface microregion. *ACS Catal.* **2021**, *11*, 1485–1494. [[CrossRef](#)]
18. Shi, H.; Fan, Z.Y.; Hong, B.; Pera-Titus, M. Aquivion perfluorosulfonic superacid as an efficient pickering interfacial catalyst for the hydrolysis of triglycerides. *ChemSusChem* **2017**, *10*, 3363–3367. [[CrossRef](#)]
19. Xi, Y.K.; Liu, B.; Wang, S.X.; Wei, S.H.; Yin, S.W.; Ngai, T.; Yang, H.Q. CO₂-responsive Pickering emulsions stabilized by soft protein particles for interfacial biocatalysis. *Chem. Sci.* **2022**, *13*, 2884–2890. [[CrossRef](#)]
20. Gaudin, P.; Jacquot, R.; Marion, P.; Pouilloux, Y.; Jérôme, F. Acid-Catalyzed Etherification of Glycerol with Long-Alkyl-Chain Alcohols. *ChemSusChem* **2011**, *4*, 719–722. [[CrossRef](#)]
21. Wu, J.; Ma, G.H. Recent studies of Pickering emulsions: Particles make the difference. *Small* **2016**, *12*, 4633–4648. [[CrossRef](#)] [[PubMed](#)]
22. Björkegren, S.; Nordstierna, L.; Törnroona, A.; Palmqvist, A. Hydrophilic and hydrophobic modifications of colloidal silica particles for Pickering emulsions. *J. Colloid. Interf. Sci.* **2017**, *487*, 250–257. [[CrossRef](#)] [[PubMed](#)]
23. Hao, Y.J.; Liu, Y.F.; Yang, R.; Jian, L.; Zhang, X.M.; Yang, H.Q. A pH-responsive TiO₂-based Pickering emulsion system for in situ catalyst recycling. *Chinese Chem. Lett.* **2018**, *29*, 778–782. [[CrossRef](#)]
24. Otero, J.; Meeker, S.; Clegg, P.S. Compositional ripening of particle-stabilized drops in a three-liquid system. *Soft Matter* **2018**, *14*, 3783–3790. [[CrossRef](#)] [[PubMed](#)]
25. Cuevas-Gómez, A.P.; González-Magallanes, B.; Arroyo-Maya, I.J.; GutiérrezLópez, G.F.; CornejoMazón, M.; Hernández-Sánchez, H. Squalene-Rich Amaranth Oil Pickering Emulsions Stabilized by Native α -Lactalbumin Nanoparticles. *Foods* **2022**, *11*, 1998. [[CrossRef](#)]
26. Hu, J.; Xu, R.Y.; Deng, W.J. Dual stabilization of Pickering emulsion with epigallocatechin gallate loaded mesoporous silica nanoparticles. *Food Chem.* **2022**, *396*, 133675. [[CrossRef](#)]
27. Nagarajan, S.; Abessolo Ondo, D.; Gassara, S.; Bechelany, M.; Balme, S.; Miele, P.; Kalkura, N.; Pochat-Bohatier, C. Porous gelatin membrane obtained from Pickering emulsions stabilized by graphene oxide. *Langmuir* **2018**, *34*, 1542–1549. [[CrossRef](#)]
28. Gonzalez-Ortiz, D.; Pochat-Bohatier, C.; Gassara, S.; Cambedouzou, J.; Bechelany, M.; Miele, P. Development of novel h-BNNS/PVA porous membranes via Pickering emulsion templating. *Green Chem.* **2018**, *20*, 4319–4329. [[CrossRef](#)]
29. Ortiz, D.G.; Pochat-Bohatier, C.; Cambedouzou, J.; Bechelany, M.; Miele, P. Pickering emulsions stabilized with two-dimensional (2D) materials: A comparative study. *Colloid Surf. A* **2019**, *563*, 183–192. [[CrossRef](#)]
30. Yang, T.Y.; Wei, L.J.; Jing, L.Y.; Liang, J.F.; Zhang, X.M.; Tang, M.; Monteiro, M.J.; Chen, Y.; Wang, Y.; Gu, S.; et al. Dumbbell-shaped bi-component mesoporous Janus solid nanoparticles for biphasic interface catalysis. *Angew. Chem. Int. Edit.* **2017**, *56*, 8459–8463. [[CrossRef](#)]
31. Hou, H.H.; Li, J.; Li, X.M.; Forth, J.; Yin, J.; Jiang, X.S.; Helms, B.A.; Russell, T.P. Interfacial Activity of Amine-Functionalized Polyhedral Oligomeric Silsesquioxanes (POSS): A Simple Strategy to Structure Liquids. *Angew. Chem.* **2019**, *131*, 10248–10253. [[CrossRef](#)]

32. Xie, D.H.; Jiang, Y.L.; Li, K.L.; Yang, X.Y.; Zhang, Y.J. Pickering emulsions stabilized by mesoporous nanoparticles with different morphologies in combination with DTAB. *ACS Omega* **2022**, *7*, 29153–29160. [[CrossRef](#)] [[PubMed](#)]
33. Kumar, H.; Dugyala, V.R.; Basavaraj, M.G. Phase Inversion of Ellipsoid-Stabilized Emulsions. *Langmuir* **2021**, *37*, 7295–7304. [[CrossRef](#)] [[PubMed](#)]
34. Li, X.; Li, J.; Gong, J.; Kuang, Y.S.; Mo, L.H.; Song, T. Cellulose nanocrystals (CNCs) with different crystalline allomorph for oil in water Pickering emulsions. *Carbohydr. Polym.* **2018**, *183*, 303–310. [[CrossRef](#)]
35. Wu, C.; Hou, D.S.; Yin, B.; Li, S.H. Synthesis and application of new core-shell structure via Pickering emulsion polymerization stabilized by graphene oxide. *Compos. Part B-Eng.* **2022**, *247*, 110285. [[CrossRef](#)]
36. Cui, D.H.; Shi, B.F.; Xia, Z.N.; Zhu, W.J.; Lu, C.L. Construction of polymer brush-decorated amphiphilic Janus graphene oxide nanosheets via a Pickering emulsion template for catalytic applications. *New J. Chem.* **2022**, *46*, 20855–20865. [[CrossRef](#)]
37. Skorupska, M.; Ilnicka, A.; Lukaszewicz, J.P. Successful Manufacturing Protocols of N-Rich Carbon Electrodes Ensuring High ORR Activity: A Review. *Processes* **2022**, *10*, 643. [[CrossRef](#)]
38. Liu, R.; Xu, Y.X.; Pu, W.F.; Shi, P.; Du, D.J.; James, J.S.; Yong, H.S. Oligomeric ethylene-glycol brush functionalized graphene oxide with exceptional interfacial properties for versatile applications. *Appl. Surf. Sci.* **2022**, *606*, 154856. [[CrossRef](#)]
39. Kim, J.; Cote, L.J.; Kim, F.; Yuan, W.; Shull, K.R.; Huang, J.X. Graphene oxide sheets at interfaces. *J. Am. Chem. Soc.* **2010**, *132*, 8180–8186. [[CrossRef](#)]
40. Gudarzi, M.M.; Sharif, F. Self assembly of graphene oxide at the liquid-liquid interface: A new route to the fabrication of graphene based composites. *Soft Matter*. **2011**, *7*, 3432–3440. [[CrossRef](#)]
41. Tang, J.; Cao, S.X.; Wang, J.L. CO₂-switchable Pickering emulsions: Efficient and tunable interfacial catalysis for alcohol oxidation in biphasic systems. *Chem. Commun.* **2019**, *55*, 11079–11082. [[CrossRef](#)] [[PubMed](#)]
42. Shan, Y.Y.; Yu, C.; Zhang, M.D.; Wei, Q.B.; An, J.L.; Lv, H.H.; Ni, L.; Qiu, J.S. Passivating the pH-Responsive Sites to Configure a Widely pH-Stable Emulsifier for High-Efficiency Benzyl Alcohol Oxidation. *ChemSusChem* **2022**, *15*, e202102473. [[CrossRef](#)] [[PubMed](#)]
43. He, Y.Q.; Wu, F.; Sun, X.Y.; Li, R.Q.; Guo, Y.Q.; Li, C.B.; Zhang, L.; Xing, F.B.; Wang, W.; Gao, J.P. Factors that affect pickering emulsions stabilized by graphene oxide. *ACS Appl. Mater. Inter.* **2013**, *5*, 4843–4855. [[CrossRef](#)]
44. Ederer, J.; Ecorchard, P.; Slušná, M.Š.; Tolasz, Z.; Smržová, D.; Lupinková, S.; Janoš, P. A Study of Methylene Blue Dye Interaction and Adsorption by Monolayer Graphene Oxide. *Adsorpt. Sci. Technol.* **2022**, *2022*, 7385541. [[CrossRef](#)]
45. Wan, W.B.; Li, L.L.; Zhao, Z.B.; Hu, H.; Hao, X.J.; Winkler, D.A.; Xi, L.C.; Hughes, T.C.; Qiu, J.S. Ultrafast fabrication of covalently cross-linked multifunctional graphene oxide monoliths. *Adv. Funct. Mater.* **2014**, *24*, 4915–4921. [[CrossRef](#)]
46. Caliman, C.C.; Mesquita, A.F.; Cipriano, D.F.; Freitas, J.C.C.; Cotta, A.A.C.; Macedo, W.A.A.; Porto, A.O. One-pot synthesis of amine-functionalized graphene oxide by microwave-assisted reactions: An outstanding alternative for supporting materials in supercapacitors. *Rsc. Adv.* **2018**, *8*, 6136–6145. [[CrossRef](#)]
47. Xue, B.; Zhu, J.G.; Liu, N.; Li, Y.X. Facile functionalization of graphene oxide with ethylenediamine as a solid base catalyst for Knoevenagel condensation reaction. *Catal. Commun.* **2015**, *64*, 105–109. [[CrossRef](#)]
48. Binks, B.P.; Lumsdon, S.O. Influence of particle wettability on the type and stability of surfactant-free emulsions. *Langmuir* **2000**, *16*, 8622–8631. [[CrossRef](#)]
49. Ou, L.L.; Song, B.; Liang, H.M.; Liu, J.; Feng, X.L.; Deng, B.; Sun, T.; Shao, L.Q. Toxicity of graphene-family nanoparticles: A general review of the origins and mechanisms. *Part. Fibre Toxicol.* **2016**, *13*, 57. [[CrossRef](#)]

Disclaimer/Publisher’s Note: The statements, opinions and data contained in all publications are solely those of the individual author(s) and contributor(s) and not of MDPI and/or the editor(s). MDPI and/or the editor(s) disclaim responsibility for any injury to people or property resulting from any ideas, methods, instructions or products referred to in the content.